Adaptive Kalman Filtering Based on Subjective Logic Self-Assessment

Thomas Griebel, Johannes Müller, Michael Buchholz, and Klaus Dietmayer

This paper has been accepted for presentation and publication at the 2024 27th International Conference on Information Fusion (FUSION), July 08 - 11, 2024, Venice, Italy. This is the accepted version of the paper, which has not been fully edited and the layout may differ from the original publication.

Citation information of the original publication:

T. Griebel, J. Müller, M. Buchholz and K. Dietmayer, "Adaptive Kalman Filtering Based on Subjective Logic Self-Assessment," 2024 27th International Conference on Information Fusion (FUSION), Venice, Italy, 2024, pp. 1-8, doi: 10.23919/FUSION59988.2024.10706328.

Adaptive Kalman Filtering Based on Subjective Logic Self-Assessment

Thomas Griebel[1], Johannes Müller[2], Michael Buchholz[1], and Klaus Dietmayer[1]

***Abstract*— Monitoring and self-assessment of tracking algorithms are essential in modern automated driving systems. However, the further use of this self-assessment information is another growing and not thoroughly studied area of research. One option is to adapt the parameters configured in the tracking algorithm online to obtain better and more robust tracking results directly. The paper proposes a novel overall concept and framework for adaptive Kalman filtering using subjective logic. Based on a self-assessment method, we present multiple variants of adaptive strategies to adapt the noise assumptions online for Kalman filtering. This paper focuses mainly on adaptation procedures for multi-sensor Kalman filters. The proposed method is evaluated in various experiments and compared with state-of-the-art adaptive Kalman filters.**

I. Introduction

In automated driving systems, involved modules are expected to react appropriately to changes in the environment. External factors range from changeable weather conditions to unexpected occurrences in urban traffic or even willful manipulation from outside. One important module in environmental perception is tracking, i.e., temporal filtering of objects measured in the vehicle's surroundings. In order to react to external changes, the tracking module needs some kind of self-assessment (SA) that monitors its performance online. Using information from this SA in tracking, filter parameters can be automatically tuned by an appropriate adaptation method, and the tracking results can be improved.

The Kalman filter (KF) [1] is the most well-known and used tracking algorithm. Since Kalman filtering was developed, adaptive Kalman filtering has been a research topic of interest. Mehra [2] already presented an overview of different approaches to adaptive filtering in 1972. He proposed a categorization of approaches into four groups: Bayesian estimation, maximum likelihood estimation, correlation methods, and covariance matching. Since then, research in this area has continued, such as [3]–[6] and surveys on noise covariance estimations, such as [7], [8]. Despite being a long-studied problem, proper adaptation mechanisms for adaptive KFs are still subject to current research, particularly since the

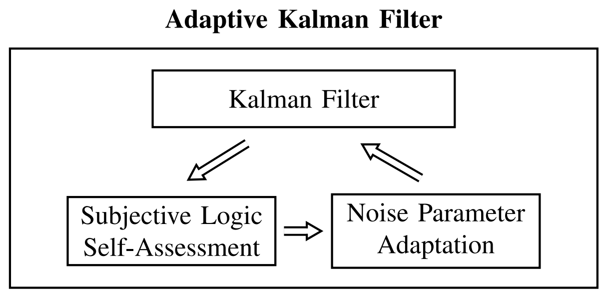

Fig. 1. The conceptual overview of our proposed adaptation approach applies an adaptation of the Kalman filter's noise parameters that makes use of a subjective logic-based self-assessment of the Kalman filter.

noise matrices are assumed to be known but usually are actually unknown [8]. In [8], the authors propose a novel optimization-based estimation scheme for the noise matrices, provide mathematical conditions for the identifiability of noise covariances, and convergence proofs. However, they do not account for adaptations based on an SA. In [9], a reinforcement learning approach is used to determine the noise parameters of a system, the unknown statistical characteristics of measurement noise. However, this requires offline training. Furthermore, in [10], an auto-tuning mechanism has recently been proposed to adapt the noise mechanisms. However, the tuning works based on the computation-heavy optimization of a hand-crafted cost function.

Adaptation is motivated by various possible issues in conventional Kalman filtering. For example, the filter usually assumes the knowledge of the process and the measurement noise. Since a priori knowledge of the time-varying noise covariance matrices is usually unavailable, the KF is not always impeccable and may even lead to filtering divergence [2]. Another possible issue, which is addressed in [11], is the so-called overshooting. This describes the procedure when a vehicle makes a turn to another direction, but the process model still keeps the position estimation along with the previous direction.

This paper presents an overall framework for adaptive Kalman filtering using SA information; see Fig. 1. We build on the SA approaches in [12]–[14] and develop the adaptation of the filter noise parameters on top of it. For this, subjective logic (SL) is used as an extension of probabilistic logic for reasoning under uncertainty [15].

Summarizing our work in this paper, we propose:

- a novel overall concept and framework of adaptive Kalman filtering based on SL,
- an adaptation strategy with multiple variants of calculating adaptation factors and estimating noise parameters,

Parts of this research have been conducted as part of the EVENTS project, which is funded by the European Union, under grant agreement No 101069614. Views and opinions expressed are however those of the author(s) only and do not necessarily reflect those of the European Union or European Commission. Neither the European Union nor the granting authority can be held responsible for them.

[1]T. Griebel, M. Buchholz, and K. Dietmayer are with the Institute of Measurement, Control, and Microtechnology, Ulm University, Germany, {firstname}.{lastname}@uni-ulm.de

[2]J. Müller was with the Institute of Measurement, Control, and Microtechnology, Ulm University, Germany, and is now with the Robert Bosch GmbH, Renningen, Germany, johanneschristian.mueller@de.bosch.com

- an extensive evaluation of various challenging experimental scenarios of our method and comparison to state-of-the-art adaptive KFs.

II. Fundamentals

This section summarizes the KF equations and the consistency examination [16], which are the basics of adaptive Kalman filtering. Then, the mathematical foundation of SL is briefly summarized [15].

A. Kalman Filter

In Kalman filtering, the central assumptions are that all models are linear and all probability densities are Gaussian. Furthermore, the process noise $\boldsymbol{v}_k \in \mathbb{R}^n$ and measurement noise $\boldsymbol{w}_k \in \mathbb{R}^m$ are uncorrelated and zero-mean Gaussian distributed. Under these conditions, it is proven that the KF [1], as a Bayes filter realization, is an optimal state estimator [17] for the state $\boldsymbol{x}_k \in \mathbb{R}^n$ using the measurements $\boldsymbol{z}_k \in \mathbb{R}^m$. The recursive equations of the KF are given by

$$\hat{\boldsymbol{x}}_{k+1|k} = \boldsymbol{F}_k \hat{\boldsymbol{x}}_k, \tag{1a}$$
$$\boldsymbol{P}_{k+1|k} = \boldsymbol{F}_k \boldsymbol{P}_k \boldsymbol{F}_k^T + \boldsymbol{Q}_k, \tag{1b}$$
$$\hat{\boldsymbol{z}}_{k+1|k} = \boldsymbol{H}_{k+1} \hat{\boldsymbol{x}}_{k+1|k}, \tag{1c}$$
$$\boldsymbol{S}_{k+1} = \boldsymbol{H}_{k+1} \boldsymbol{P}_{k+1|k} \boldsymbol{H}_{k+1}^T + \boldsymbol{R}_{k+1}, \tag{1d}$$
$$\boldsymbol{K}_{k+1} = \boldsymbol{P}_{k+1|k} \boldsymbol{H}_{k+1}^T \boldsymbol{S}_{k+1}^{-1} \tag{1e}$$
$$\hat{\boldsymbol{x}}_{k+1} = \hat{\boldsymbol{x}}_{k+1|k} + \boldsymbol{K}_{k+1} \boldsymbol{\gamma}_{k+1}, \tag{1f}$$
$$\boldsymbol{P}_{k+1} = \boldsymbol{P}_{k+1|k} + \boldsymbol{K}_{k+1} \boldsymbol{S}_{k+1} \boldsymbol{K}_{k+1}^T, \tag{1g}$$

where $\boldsymbol{F}_k \in \mathbb{R}^{n\times n}$ is the process matrix, $\boldsymbol{H}_{k+1} \in \mathbb{R}^{m\times n}$ the measurement matrix, and $\hat{\boldsymbol{x}}_{k+1|k} \in \mathbb{R}^n$ and $\hat{\boldsymbol{z}}_{k+1|k} \in \mathbb{R}^m$ are the state and measurement prediction. Also, k denotes the time step index for the underlying constant sample time. Furthermore, $\boldsymbol{P}_{k+1|k} \in \mathbb{R}^{n\times n}$ is the covariance matrix of the predicted state, $\boldsymbol{Q}_k = \mathbb{E}\left[\boldsymbol{v}_k \boldsymbol{v}_k^T\right] \in \mathbb{R}^{n\times n}$ the covariance matrix of the process noise, and $\boldsymbol{R}_{k+1} = \mathbb{E}\left[\boldsymbol{w}_{k+1} \boldsymbol{w}_{k+1}^T\right] \in \mathbb{R}^{m\times m}$ the covariance matrix of the measurement noise. Using the innovation covariance matrix $\boldsymbol{S}_{k+1} \in \mathbb{R}^{m\times m}$ and the Kalman gain $\boldsymbol{K}_{k+1} \in \mathbb{R}^{n\times m}$, the estimated covariance matrix $\boldsymbol{P}_{k+1} \in \mathbb{R}^{n\times n}$ is obtained in the update step. Moreover, in the update step, the estimated state $\hat{\boldsymbol{x}}_{k+1}$ is computed via Kalman gain and residual

$$\boldsymbol{\gamma}_{k+1} := \boldsymbol{z}_{k+1} - \hat{\boldsymbol{z}}_{k+1|k}. \tag{2}$$

In practice, however, the Gaussian assumption only holds approximately, and $\boldsymbol{Q}$ and $\boldsymbol{R}$ are not known exactly Hence, the optimality, consistency, and unbiasedness are no longer given. To test for the latter two properties, the normalized estimation error squared (NEES)

$$\varepsilon_{\boldsymbol{x}_k} = \tilde{\boldsymbol{x}}_k^T \boldsymbol{P}_k^{-1} \tilde{\boldsymbol{x}}_k \tag{3}$$

can be applied using the state residual $\tilde{\boldsymbol{x}}_k := \boldsymbol{x}_k - \hat{\boldsymbol{x}}_{k|k}$, which, however, requires ground truth (GT) data. If all assumptions of the KF are met, the NEES is χ^2 distributed with n degrees of freedom. The NEES value is expected to be inside a particular confidence interval of the χ^2 distribution to examine consistency.

B. Subjective Logic

The key component of SL is the so-called opinions [15]. With these, SL can explicitly model the statistical uncertainty, comparable to the Dempster-Shafer theory [18], [19]. However, SL provides a comprehensive and flexible fusion framework with several operators to fuse and merge opinions, like the cumulative belief fusion (CBF) and the averaging belief fusion (ABF) [20], [21], depending on the fusion task. This comprehensive fusion framework is a major benefit of SL. For more details about the fusion operator and when to use which, see [15].

Information about belief, uncertainty, and base rate of a discrete random variable X is represented in SL by a multinomial opinion ω_X.

Definition 1 (Multinomial Opinion)**.** *Consider a random variable X in the finite domain $\mathbb{X}$ with cardinality $W = |\mathbb{X}| \geq 2$. A multinomial opinion is then defined as $\omega_X = (\boldsymbol{b}_X, u_X, \boldsymbol{a}_X)$ with*

$$\boldsymbol{b}_X(x) : \mathbb{X} \mapsto [0,1], \qquad 1 = u_X + \sum_{x\in\mathbb{X}} \boldsymbol{b}_X(x)\,, \tag{4a}$$
$$\boldsymbol{a}_X(x) : \mathbb{X} \mapsto [0,1], \qquad 1 = \sum_{x\in\mathbb{X}} \boldsymbol{a}_X(x)\,. \tag{4b}$$

The belief mass distribution $\boldsymbol{b}_X$ over $\mathbb{X}$ models the belief in each event, the uncertainty mass $u_X \in [0,1]$ forms the lack of evidence, and the base rate distribution $\boldsymbol{a}_X$ over $\mathbb{X}$ represents the prior probability for each event.

The projected probability can be used to map a multinomial opinion to a classical probability distribution. This is done by

$$\boldsymbol{P}_X(x) = \boldsymbol{b}_X(x) + \boldsymbol{a}_X(x) u_X, \quad \forall x \in \mathbb{X}. \tag{5}$$

In the classical probability space, the projected probability equals the expected outcome of the opinion.

To compare two opinions about the same variable X, their distance can be measured by the degree of conflict (DC) [15].

Definition 2 (Degree of Conflict)**.** *Consider two multinomial opinions ω_X^A and ω_X^B of source A and B over $X \in \mathbb{X}$. The* DC $\in [0,1]$ *between two opinions ω_X^A, ω_X^B is computed by*

$$\mathrm{DC}\left(\omega_X^A, \omega_X^B\right) = \mathrm{PD}\left(\omega_X^A, \omega_X^B\right) \cdot \mathrm{CC}\left(\omega_X^A, \omega_X^B\right), \tag{6}$$

using the projected distance $\mathrm{PD}\left(\omega_X^A, \omega_X^B\right) = \frac{1}{2}\sum_{x\in\mathbb{X}} |\boldsymbol{P}_X^A(x) - \boldsymbol{P}_X^B(x)| \in [0,1]$ *and the conjunctive certainty* $\mathrm{CC}\left(\omega_X^A, \omega_X^B\right) = \left(1 - u_X^A\right)\left(1 - u_X^B\right) \in [0,1]$.

A small DC signifies that the opinions are similar, while a large DC signifies that they are different.

III. Adaptation Strategy for Kalman Filtering Using Subjective Logic

The general adaptation strategy consists of four major steps: The SA module, the generation of multiple parameter hypotheses with corresponding additional SA measures, a situation analysis based on the SA measures, and a focused adaptation of the corresponding noise parameters. This section details these four steps.

A. Self-Assessment Measures

First, the SA for Kalman filtering, as presented in [12], [14], is applied to calculate the basic single-sensor quality measures with corresponding explicit uncertainties. This means we obtain SA scores in each time step for every sensor $s \in \{1, \dots, V\}$. These consist of the quality measure, the uncertainty, and the threshold, i.e.,

$$\left(\delta^{(s)}, u_X^{(s)}, \eta^{(s)}\right), \quad s = 1, \dots, V \tag{7}$$

based on the SL opinions $\omega_X^{(s)}$ for each sensor s. Performing the SA procedure from [12] for all V sensors, the tuple of all single-sensor SA measures is obtained in vector notation $(\boldsymbol{\delta}, \boldsymbol{u}, \boldsymbol{\eta})$. The quality measures $\delta^{(s)}$ are calculated using the DC operator, the obtained SA opinion $\omega_X^{(s)}$, and its reference opinion $\omega_{X_{\text{ref}}}^{(s)}$, modeling the initial KF assumptions, such that

$$\delta^{(s)} = \text{DC}\left(\omega_X^{(s)}, \omega_{X_{\text{ref}}}^{(s)}\right), \quad s = 1, \dots, V. \tag{8}$$

The corresponding explicit uncertainty of the quality measure follows directly from $\omega_X^{(s)}$ and is given by $u^{(s)} = u_X^{(s)}$. In addition, the corresponding threshold $\eta^{(s)}$ is also calculated using $\omega_X^{(s)}$ and a chosen confidence level $\alpha \in [0, 1]$ using the threshold calculation proposed in [13].

In addition, we can also calculate the DC between SA opinions of different sensors s_1, $s_2 \in \{1, \dots, V\}$. Thus, we obtain additional comparison measures

$$\delta^{(s_1,s_2)} = \text{DC}\left(\omega_X^{(s_1)}, \omega_X^{(s_2)}\right) \quad \forall s_1, s_2 = 1, \dots, V \tag{9}$$

between each two sensors with $s_1 \neq s_2$. Then, the overall SA matrix $\boldsymbol{\Delta} = \left(\delta^{(s_1,s_2)}\right) \in [0, 1]^{V \times V}$ is obtained for a certain time step based on all sensors. Due to the commutative property of the DC operator, the matrix is symmetric. For more information on the SA algorithm, please refer to [12].

B. Hypotheses Generation

We use multiple hypotheses to gain more information for the situation analysis to generate further quality measures and to ensure a focused adaptation procedure. Following the same process for obtaining the SA measures in the overall SA matrix $\boldsymbol{\Delta}$, we can compare the assumptions of the KF noise parameters with different hypotheses. These hypotheses can be, for example, various noise parameters, e.g., with smaller and higher values. The hypotheses generation approach can be implemented by using related reference opinions $\omega_{X_{\text{ref},\theta}}^{(s)}$ for each additional hypotheses $\theta \in \{1, \dots, H\}$. This yields to an SA hypotheses vector $\boldsymbol{\delta}_\theta \in [0, 1]^V$ with

$$\boldsymbol{\delta}_\theta = \begin{bmatrix} \delta_\theta^{(1)} \\ \vdots \\ \delta_\theta^{(V)} \end{bmatrix} = \begin{bmatrix} \text{DC}\left(\omega_X^{(1)}, \omega_{X_{\text{ref},\theta}}^{(1)}\right) \\ \vdots \\ \text{DC}\left(\omega_X^{(V)}, \omega_{X_{\text{ref},\theta}}^{(V)}\right) \end{bmatrix}, \quad \theta = 1, \dots, H. \tag{10}$$

For example, we can generate two hypotheses about the assumed noise parameter. First, the assumed noise parameter has a smaller value. Second, the assumed noise parameter has a higher value.

C. Situation Analysis

Using all the SA information we have obtained so far, we perform a general situation analysis of the components contributing to the filter algorithm's performance. Our proposed situation analysis is based on majority voting, which is most common in the area of security (*honest majority* assumption, see e.g. [22]). Applied to our adaptive KF, this means that most of our system's relevant components (the sensors/measurements and the process models) keep working correctly in case some become unreliable and thus require adaptations. We consider two main cases in our adaptation strategy: Measurement noise adaptation of selected sensors and process noise adaptation.

1) Measurement Noise Adaptation: This case covers the situation where at least one sensor SA measure reports a violation, while the majority of sensors still meet the measurement and process model assumptions and provide data coherent with each other. This case is formulated by

$$0 < \sum_{s=1}^{V} \mathbb{1}_{\left\{\delta^{(s)} > \eta^{(s)}\right\}} \leq \frac{V}{2} \tag{11}$$

with the indicator function $\mathbb{1}$, which is 1 if $\delta^{(s)} > \eta^{(s)}$ and 0 otherwise. The corresponding measurement covariance matrices, which represent the noise assumption for the sensor behavior, will then be adapted. To do this, we find the indices of the SA measures that are greater than their thresholds, i.e.,

$$s^\star \in \mathbb{S}^\star : \delta^{(s^\star)} > \eta^{(s^\star)}. \tag{12}$$

We can either decrease or increase their measurement noise for the selected sensors $\mathbb{S}^\star$. This choice can be made using the SA measures $\boldsymbol{\delta}_\theta$ based on our generated hypotheses $\theta = 1, \dots, H$ in (10), applying one of the methods presented in the following Sections IV-A, IV-B, and IV-C. Or we directly estimate the noise parameter as proposed in Section IV-D.

2) Process Noise Adaptation: In case our SA observes that more than half of the sensors deviate from the filter's expectation but are consistent among themselves, we conclude that the process model noise assumptions might be wrong. This case is identified by

$$\sum_{s_1=1}^{V} \sum_{s_2=s_1+1}^{V} \mathbb{1}_{\left\{\delta^{(s_1,s_2)} > \min\left\{\eta^{(s_1)}, \eta^{(s_2)}\right\}\right\}} < V/2 < \sum_{s=1}^{V} \mathbb{1}_{\left\{\delta^{(s)} > \eta^{(s)}\right\}}. \tag{13}$$

As in (12), we find the sensors $\mathbb{S}^\star$ reporting a violation and modify the noise of the process model with an appropriate adaptation factor based on their SA measures. This is shown in the following sections.

The output of the situation analysis module is the analyzed situation $C \in \mathbb{C}$, where $\mathbb{C}$ is the space of all possible situations. The obtained situation C is then used in the subsequent noise parameter adaptation. Thus, in the following sections, we focus on the choice and the calculation of an adaptation factor or the noise parameter estimation itself.

Algorithm 1 General proposed adaptation strategy.

Input: Noise covariance matrices of the Kalman filter for the process model $\boldsymbol{Q}$ and for the measurement models $\boldsymbol{R}^{(s)}$ of the sensors $s = 1, \dots, V$

Output: Adjusted noise covariance matrices $\tilde{\boldsymbol{Q}}$ and $\tilde{\boldsymbol{R}}^{(s)}$ of the sensors $s = 1, \dots, V$

procedure ADAPTATION $(\boldsymbol{Q}, \boldsymbol{R}^{(1)}, \dots, \boldsymbol{R}^{(V)})$
  $(\boldsymbol{\delta}, \boldsymbol{u}, \boldsymbol{\eta})$, $\boldsymbol{\Delta} \leftarrow$ SA procedure from [12], [14] for all V sensors
  $(\boldsymbol{\delta}_1, \dots, \boldsymbol{\delta}_H) \leftarrow$ SA measures of H further generated hypotheses θ
  $C \leftarrow$ Situation analysis using $(\boldsymbol{\delta}, \boldsymbol{u}, \boldsymbol{\eta})$, $\boldsymbol{\Delta}$, and $(\boldsymbol{\delta}_1, \dots, \boldsymbol{\delta}_H)$
  $\tilde{\boldsymbol{Q}}, \tilde{\boldsymbol{R}}^{(1)}, \dots, \tilde{\boldsymbol{R}}^{(V)} \leftarrow$ Noise parameter adaptation procedure from either Section IV-A, IV-B, IV-C or IV-D based on all obtained information C, $(\boldsymbol{\delta}, \boldsymbol{u}, \boldsymbol{\eta})$, $\boldsymbol{\Delta}$, and $\boldsymbol{Q}, \boldsymbol{R}^{(1)}, \dots, \boldsymbol{R}^{(V)}$
  return $\tilde{\boldsymbol{Q}}, \tilde{\boldsymbol{R}}^{(1)}, \dots, \tilde{\boldsymbol{R}}^{(V)}$
end procedure

D. Noise Parameter Adaptation

Finally, we adapt or auto-tune the measurement and process noise. For this, we propose four different noise parameter adaptation approaches described in Section IV. The proposed adaptation procedure is summarized in Algorithm 1.

IV. NOISE PARAMETER ADAPTATION APPROACHES

Based on different basic assumptions and thus aiming at solutions for different situations, we propose four variants of the noise parameter adaptation step. The first approach uses a constant adaptation factor exploiting expert knowledge about the whole system. In particular, when the consequences of violating the assumptions are known, a specific choice of adaptation factor can be made. The second adaptation approach is based on SL's trust revision (TR) concept [23]. It is a conservatively designed method for situations where caution is more important than dynamics, like situations where only outliers and no jumps are expected. Furthermore, the method based on the TR and uncertainty differential (UD) [15] concepts is designed for situations with high dynamics, e.g., for frequently jumping parameters. With the additional use of the UD concept, the more surprising a significant disturbance is, the faster the response can be to the desired extent. Last but not least, the proposed hybrid method with classical parameter estimation using the SL-based SA method combines the aspects of high dynamics and high precision. Therefore, the hybrid method is advantageous in most situations but also computationally more complex than the others.

A. Constant Adaptation Factor

The constant adaptation factor strategy is particularly useful to incorporate expert knowledge like estimates of how system changes affect the noise parameters. For example, for a one-dimensional measurement noise parameter $w \sim \mathcal{N}\left(0, \sigma^2\right)$, the constant factor is a scalar $\beta > 0$ and yields the adaptation of the noise parameter $\tilde{\sigma} = \beta\,\sigma$. More generally, the adaptation can be expressed as

$$\tilde{\boldsymbol{Q}} = \boldsymbol{B}_{\boldsymbol{Q}}\,\boldsymbol{Q}, \tag{14a}$$

$$\tilde{\boldsymbol{R}}^{(s)} = \boldsymbol{B}_{\boldsymbol{R}^{(s)}}\,\boldsymbol{R}^{(s)}, \tag{14b}$$

using the KF process and measurement noise covariance matrices introduced in Section II-A. Here, $\boldsymbol{B}_{\boldsymbol{Q}} \in \mathbb{R}_{>0}^{n \times n}$ with $\boldsymbol{B}_{\boldsymbol{Q}} = \left(b_{ij}^{\boldsymbol{Q}}\right)$ and $\boldsymbol{B}_{\boldsymbol{R}^{(s)}} \in \mathbb{R}_{>0}^{m \times m}$ with $\boldsymbol{B}_{\boldsymbol{R}^{(s)}} = \left(b_{ij}^{\boldsymbol{R}^{(s)}}\right)$ contain expert knowledge about possible system changes. The types of matrices $\boldsymbol{B}_{\boldsymbol{Q}}$ and $\boldsymbol{B}_{\boldsymbol{R}^{(s)}}$ depend strongly on the noise covariance matrices $\boldsymbol{Q}$ and $\boldsymbol{R}^{(s)}$. For example, if $\boldsymbol{Q}$ and $\boldsymbol{R}^{(s)}$ are diagonal matrices, then $\boldsymbol{B}_{\boldsymbol{Q}}$ and $\boldsymbol{B}_{\boldsymbol{R}^{(s)}}$ should also be diagonal. This would mean that each diagonal component for $i = 1, \dots n$ and $j = 1, \dots, m$ of the noise covariance matrices can be adjusted by the constant factors $b_{ii}^{\boldsymbol{Q}} > 0$ and $b_{jj}^{\boldsymbol{R}^{(s)}} > 0$, respectively. Here, $b_{ii}^{\boldsymbol{Q}}, b_{jj}^{\boldsymbol{R}^{(s)}} \in (0, 1)$ means a decrease in the noise covariance matrix component and $b_{ii}^{\boldsymbol{Q}}, b_{jj}^{\boldsymbol{R}^{(s)}} > 1$ an increase.

However, in a more general setting, this mechanism is often not flexible enough. Therefore, further adaptation mechanisms using specific assessment measures, their explicit uncertainty, and certain concepts from SL are proposed.

B. Adaptation Factor Based on Trust Revision

The original motivation for the concept of TR [15] is that when multiple sources have conflicting opinions, at least one of the sources is not reliable [23]. Thus, a revision factor (RF) for the corresponding source is computed depending on the DC values of the other sources to reduce the trust in the source. By applying TR in the adaptation strategy, an RF can be calculated to selectively adjust the noise parameters. Using $s^\star \in \mathbb{S}^\star$ from (12), the RF is computed similarly to [23] via the maximum conflict (MC), the average conflict (AC), and the revision weight (RW):

$$\mathrm{MC}\left(\omega_X^{(\mathbb{S}^\star)}\right) = \max_{s^\star \in \mathbb{S}^\star} \delta^{(s^\star)}, \tag{15a}$$

$$\mathrm{AC}\left(\omega_X^{(\mathbb{S}^\star)}\right) = \frac{1}{|\mathbb{S}^\star|} \sum_{s^\star \in \mathbb{S}^\star} \delta^{(s^\star)}, \tag{15b}$$

$$\mathrm{RW}\left(\omega_X^{(s^\star)}\right) = \begin{cases} \frac{\mathrm{MC}\left(\omega_X^{(\mathbb{S}^\star)}\right)\,\tilde{d}}{\mathrm{MC}\left(\omega_X^{(\mathbb{S}^\star)}\right) - \mathrm{AC}\left(\omega_X^{(\mathbb{S}^\star)}\right)} & , \ \tilde{d} > 0 \\ 0 & , \ \text{else} \end{cases} \tag{15c}$$

with $\tilde{d} := \delta^{(s^\star)} - \mathrm{AC}\left(\omega_X^{(\mathbb{S}^\star)}\right)$. This yields the RF

$$\mathrm{RF}\left(\omega_X^{(s^\star)}\right) = \left(1 - \mathrm{RW}\left(\omega_X^{(s^\star)}\right)\right) \tag{16}$$

to decrease the noise parameter, while the reciprocal of (16) is used to increase the noise parameter. The decision to increase or decrease is determined by the result of the situation analysis C. The presented procedure for calculating the RF must be performed for each noise parameter component that can be mapped onto the measurement space and should be adaptable so that all the corresponding RFs can be gathered in an adaptation factor matrix. Consequently, this results in the mathematical formulation of the noise parameter adaptation with respect to the KF process and the measurement noise parameters, namely

$$\tilde{\boldsymbol{Q}} = \mathrm{RF}_{\boldsymbol{Q}}^{\mathrm{TR}}\, \boldsymbol{Q}, \tag{17a}$$

$$\tilde{\boldsymbol{R}}^{(s)} = \mathrm{RF}_{\boldsymbol{R}^{(s)}}^{\mathrm{TR}}\, \boldsymbol{R}^{(s)}, \tag{17b}$$

where the matrices $\mathrm{RF}_{\boldsymbol{Q}}^{\mathrm{TR}} \in \mathbb{R}_{>0}^{n\times n}$ and $\mathrm{RF}_{\boldsymbol{R}^{(s)}}^{\mathrm{TR}} \in \mathbb{R}_{>0}^{m\times m}$ denote that each noise component can be adapted by an adaptation factor calculated based on the TR concept.

As mentioned, this conservative strategy is particularly useful if the focus is on the avoidance of false positives. However, if dynamics are more important, the explicit uncertainty measure $\boldsymbol{u}$ of the SA module can be used additionally to calculate adaptation factors.

C. Adaptation Factor Based on Trust Revision and Uncertainty Differential

In SL, it can be discussed whether the obtained explicit uncertainty is sufficiently taken into account. By extending the RF from (16) with the concept of UD introduced in [15], more weight can be given to the explicit uncertainty, i.e.,

$$\mathrm{RF}\left(\omega_X^{(s^\star)}\right) = \left(1 - \mathrm{RW}\left(\omega_X^{(s^\star)}\right)\right) \cdot \left(1 - \mathrm{UD}\left(\omega_X^{(s^\star)}\right)\right), \tag{18}$$

where the UD of the selected sensor opinion is defined as

$$\mathrm{UD}\left(\omega_X^{(s^\star)}\right) = \frac{u_X^{(s^\star)}}{\sum\limits_{s\in\mathbb{S}^\star\setminus\{s^\star\}} u_X^{(s)}}\,. \tag{19}$$

Again, (18) is the formula for reducing while taking its reciprocal increases the noise parameters. This decision is again based on the result C of the situation analysis.

As before, the presented procedure for calculating the RF in (18) must be performed for each noise parameter component. This leads to the replacement of $\mathrm{RF}_{\boldsymbol{Q}}^{\mathrm{TR}}$ and $\mathrm{RF}_{\boldsymbol{R}^{(s)}}^{\mathrm{TR}}$ in (17) by $\mathrm{RF}_{\boldsymbol{Q}}^{\mathrm{TR-UD}} \in \mathbb{R}_{>0}^{n\times n}$ and $\mathrm{RF}_{\boldsymbol{R}^{(s)}}^{\mathrm{TR-UD}} \in \mathbb{R}_{>0}^{m\times m}$. The index of the RF matrix denotes that each noise component is adapted by an adaptation factor calculated based on the TR and UD concepts.

D. Classical Noise Parameter Estimation Based on Subjective Logic Self-Assessment

In contrast to the previously presented strategies for calculating the adaptation factor in closed-form using SL theory, we now combine the SL-based SA with classical noise parameter estimation. The core idea of this approach is to use the already computed dynamic time intervals of consistency of the SA. For details on the dynamic time intervals of consistency, see [12]. Then, we are able to precisely estimate the noise parameters based on these time intervals of consistency. When there has not been a change in the GT parameters for a long time, we are able to use a long-term time window for precise estimation, with many samples over that related time interval. In contrast, we can react quickly and use only the samples of the current short-term consistency window, where the change is already included in the noise parameter estimation, in case of a sudden change in the GT parameters.

We use the noise parameter estimates proposed in [8] for classical noise parameter estimation. For estimating the actual measurement noise covariance matrix $\tilde{R}$, we use the relation [8]

$$\tilde{\boldsymbol{R}}_k = \left(\boldsymbol{I}_{n_z} - \boldsymbol{H}_k \boldsymbol{K}_k\right) \tilde{\boldsymbol{S}}_k. \tag{20}$$

Here, $\tilde{\boldsymbol{S}}_k$ is the estimated actual innovation covariance, which can be calculated over a time interval with $N \in \mathbb{N}$ samples [24], [25] such that

$$\tilde{\boldsymbol{S}}_k = \frac{1}{N} \sum_{j=k-N}^{k} \boldsymbol{\gamma}_j \boldsymbol{\gamma}_j^T. \tag{21}$$

Estimating $\boldsymbol{R}_k$ by $\tilde{\boldsymbol{R}}_k$ in (20) can be reasoned by utilizing the post-fit residual $\boldsymbol{\mu}_k = \boldsymbol{z}_k - \boldsymbol{H}_k \hat{\boldsymbol{x}}_{k|k}$ and the innovation sequence $\boldsymbol{\gamma}_k = \boldsymbol{z}_k - \boldsymbol{H}_k \hat{\boldsymbol{x}}_{k|k-1}$ from (2). For the detailed derivation, see [8].

Furthermore, the actual process noise covariance matrix can be estimated using [8]

$$\tilde{\boldsymbol{Q}}_k = \boldsymbol{P}_{k+1|k+1} + \boldsymbol{K}_k \tilde{\boldsymbol{S}}_k \boldsymbol{K}_k^T - \boldsymbol{F}_k \boldsymbol{P}_{k|k} \boldsymbol{F}_k^T\,. \tag{22}$$

For both estimates in (20) and (22), note that the estimated actual innovation covariance matrix $\tilde{\boldsymbol{S}}_k$ in (21) is needed.

In our method, the noise covariance estimates are not computed based on a fixed sliding window of interval length $N \in \mathbb{N}$ as in most of the literature such as [24], [25], but on the dynamically obtained window of consistency $\boldsymbol{n}^\star \in \mathbb{N}^{V+1}$ resulting from the short-term and long-term memory fusions. This is obtained in the SA procedure by focusing on whether there have been any parameter changes, i.e.,

$$n^\star(\omega_X) = \begin{cases} n_{\mathrm{lt}}(\omega_X) + n_{\mathrm{st}}(\omega_X) & \text{, consistent} \\ n_{\mathrm{st}}(\omega_X) & \text{, else.} \end{cases} \tag{23}$$

Then, we can specifically adjust the respective sensor or process model, each of which has certain determined dynamic consistency time windows $n^\star\left(\omega_X^{(s)}\right)$ and process model $n^\star\left(\omega_X^{(\boldsymbol{Q})}\right)$. This is mainly obtained by using our proposed situation analysis in Section III-C. This yields the consistency time window vector

$$\boldsymbol{n}^\star\left(\omega_X\right) = \left[n^\star\left(\omega_X^{(1)}\right), \ldots, n^\star\left(\omega_X^{(V)}\right), n^\star\left(\omega_X^{(\boldsymbol{Q})}\right)\right]^T. \tag{24}$$

V. Experiments

To evaluate our proposed SL-based adapters, we construct challenging simulation scenarios. First, we evaluate all our adapter variants on a scenario with a jump in the GT measurement noise parameters. Second, we also consider state-of-the-art adaptive KFs as references and compare these with our most promising adaptation method. The scenario that is hereby considered contains various disturbances in the GT measurement noise of the disturbed sensor. Third,

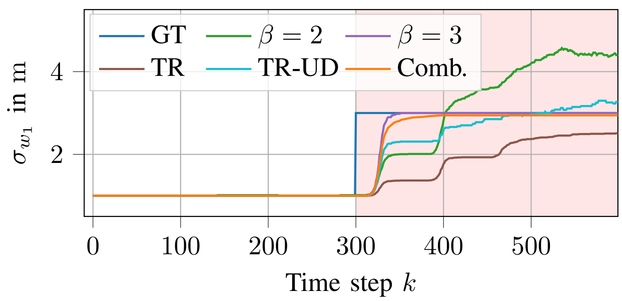

Fig. 2. Measurement noise parameters of a three-sensor simulation scenario with a factor 3 jump in the measurement noise of sensor 1 at time step 300. The SL-based adaptation approaches aim to correctly adapt the GT measurement noise. The red shadow indicates the disturbance.

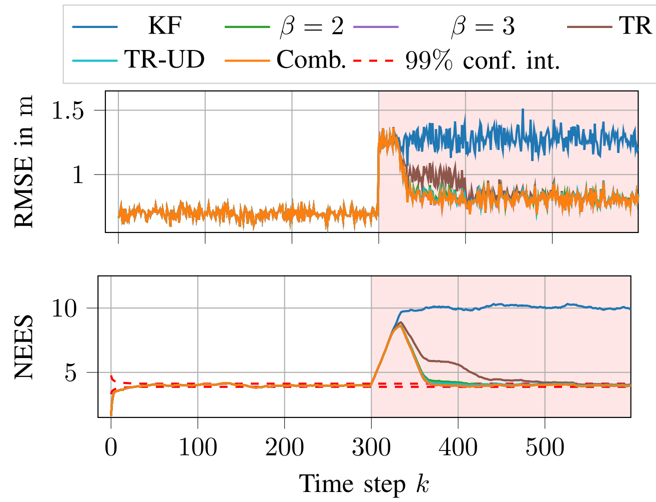

Fig. 3. Results of the SL-based adaptation approaches in a linear simulation scenario with 3 sensors and one disturbance in the measurement noise of sensor 1. The adaptation methods aim to reduce the positional RMSE and keep the time-averaged NEES in its confidence interval. The red shadow indicates the perturbation time interval.

process noise disturbances are considered, which shows that our proposed adapter is also able to identify and deal with these kinds of fault events.

In all scenarios, we consider a multi-sensor single-object simulation setup where a single object is tracked using three sensors, which each measure the position in two dimensions $(x, y) \in \mathbb{R}^2$. Initially, all sensors are assumed equal, i.e., $w_k \sim N(0, \boldsymbol{R})$ with constant variance $\sigma_w > 0$ for all sensors. In addition, a white noise acceleration model is assumed with initial time-invariant process noise $v_k \sim N(0, \boldsymbol{Q})$ with constant variance $\sigma_v > 0$. This initial setup satisfies the KF's assumptions, so no initial adaptation is needed. All results are the averaged values of 100 Monte Carlo runs.

A. Comparison of Subjective Logic-Based Adapters

First, the four variants of the proposed SL-based adapters are evaluated on a basic simulation scenario with one disturbed sensor. The disturbance manifests as a jump in the GT measurement noise by a factor of 3 at simulation time step 300. The GT measurement noise for sensor 1, as well as the adapted measurement noises performed by the adaptation method with the constant adaptation factors $\beta = 2$ and $\beta = 3$, the method based on TR, the approach based on TR and UD, and the combined method (abbreviated with comb.) are shown in Fig. 2. Unsurprisingly, for the other two sensors as well as for the process noise, all methods correctly estimated the noise parameters with the same performance and are hence omitted. All SL-based adaptation approaches react in the measurement noise of sensor 1 after a certain time interval of about 20 time steps, which is the time period the methods need to decide and adjust the correct noise parameter. The constant adaptation factor $\beta = 2$ overshoots the targeted GT measurement noise of 3 since a correct adaptation is impossible for this case, while the perfectly chosen factor $\beta = 3$ yields an optimal adaptation to the desired level. The slow increase in the noise parameter estimation of the TR method is very conservative. On the other hand, the TR-UD adjustment is more dynamic but slightly overshoots the GT. The combined method using the SL-based SA and classical noise parameter estimation shows good results in noise adaptation, almost as accurate as the perfectly chosen constant factor of 3.

The GT-based evaluation measures for the comparison scenario of the SL-based adaptive KFs are shown in Fig. 3. Here, the same discussion can be made as before for the adaptation of the noise parameters between the different SL-based approaches. It can be seen that all adapters improve the results in terms of RMSE and NEES. In the RMSE and NEES plots, the difference between the methods with constant adaptation factor $\beta = 3$, the TR-UD, and the combined approach is small. In fact, the plots superimpose so that only the last plotted combined method is visible. It is worth noting that for the NEES, all of the proposed adaptation methods eventually come back inside the confidence interval, so consistency is again ensured despite the noise parameter perturbation. For a more detailed analysis, the average positional RMSE has been evaluated before the jump (time steps $0-300$) and after it (time steps $300-600$). In the first time interval, all adapters and the standard KF obtain $0.696\,\mathrm{m}$, which is the optimal result. After that, the standard KF, the adapter with $\beta = 2$, with $\beta = 3$, the TR adapter, the TR-UD adapter, and the combined method obtain an RMSE of $1.277\,\mathrm{m}$, $0.876\,\mathrm{m}$, $0.863\,\mathrm{m}$, $0.914\,\mathrm{m}$, $0.869\,\mathrm{m}$, and $0.864\,\mathrm{m}$, respectively. Hence, all adapters reduce the RMSE of the standard KF, while the difference between the optimally chosen constant adaptation factor of $\beta = 3$ with the best performance and the combined method is only one hundredth. Hence, since the combined approach is more generally applicable, the combined method is chosen as the SL-based adaptation method for further comparison.

B. Disturbance in Measurement Noise

In the next step, we compare our method to the covariance adjustment (CA) adapter [3], the robust innovation-based (RIAE) adapter [4], and fuzzy aided (FL) adapter [5], which are state-of-the-art adaptive KFs. Since the reference methods are not able to adjust measurement and process

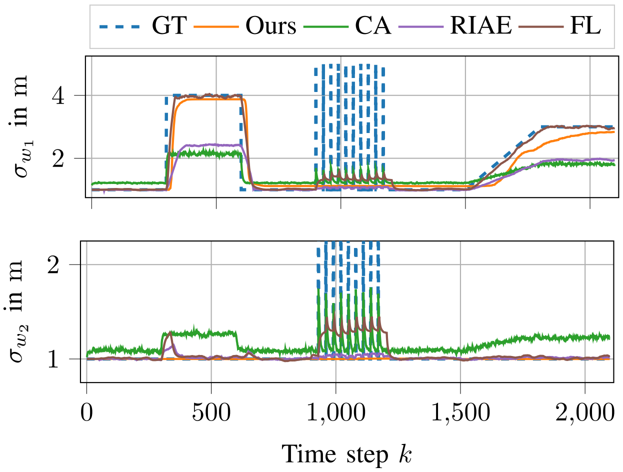

Fig. 4. Measurement noise parameters of the disturbance scenario in the measurement noise of sensor 1. The adaptation approaches aim to correctly adapt the GT measurement noise. The red shadows indicate the disturbances.

noise simultaneously, we limit the comparison to adjusting the measurement noise. For this, we consider a three-sensor simulation scenario, in which a jump of factor 4 takes place in sensor 1, then several measurement outliers of factor 5 occur every 30 time steps for all sensors at intervals of 10 time steps between the sensors, and finally a drift to the level of 3 times the original noise level increases the measurement noise. Fig. 4 visualizes the scenario. The measurement noise of sensor 3 is not plotted here because it shows results that are basically identical to sensor 2. In general, all adapters adjust the measurement noise of the sensor 1. However, the CA and RIAE adapters do not reach the jump and drift disturbance level. The CA adapter performs well during the outlier disturbances. The FL and our proposed SL adapters reach the disturbance level of the jump and the drift. Here, the FL adapter is even slightly faster than the SL adapter. During the outlier disturbance, the SL adapter does not react at all. This is intended here, because the adapter is designed to not react to single outliers but to continuous statically significant changes in the noise parameters. For sensor 2 and sensor 3, the comparison adapters adjust the noise parameters even during the jump and drift disturbance of sensor 1, but nothing changes in the current sensor. In contrast, the SL adapter correctly does not adjust the parameters. The same aspects can be seen in the RMSE results of the adapters compared to the KF with constant noise parameters in Fig. 5. The NEES results are not plotted here because they show similar results as the RMSE plot. The averaged values of the RMSE results over corresponding time intervals are summarized in Table I. Of all the adapters, the one with the best performance is highlighted in bold, and the one with the second-best performance is underlined. This indicates the strength of the different adapters. Overall, our proposed SL-based adapter outperforms the comparison adapters in most of the time intervals.

C. *Disturbance in Process Noise*

Since the other adaptive KFs cannot adjust both measurement and process noise, the proposed SL-based adapter is only compared with the standard KF for the evaluation of process noise disturbances. Fig. 6 shows the GT error evaluation measures for a scenario in which the process noise $\sigma_{v_{\text{vel}}}$ is stepped from $0.5\,\text{m}\,\text{s}^{-2}$ to $2.0\,\text{m}\,\text{s}^{-2}$ at time step 300. For this scenario, the adapter needs a short delay of 30 time steps to decide on the adaptation. The RMSE value can be significantly reduced using the SL adapter. Before the jump, both our method and the KF have a positional RMSE of $0.701\,\text{m}$, which increases due to the jump to $1.169\,\text{m}$ for the KF and $0.869\,\text{m}$ for our method. In total, over all time steps, the KF has an RMSE of $0.935\,\text{m}$, while our method only has an RMSE of $0.785\,\text{m}$. In the NEES plot, the SL adapter can significantly improve the consistency compared to the standard KF. However, even the SL method has also difficulty ensuring that the NEES value returns to its confidence interval. This also shows that a process noise disturbance is a challenging and sensitive task.

VI. Conclusion

In this work, we proposed an overall adaptation framework for Kalman filtering based on the SL theory. As a fundamental part, we use our developed SL-based SA approach to make a situation analysis to focus on adapting the noise parameters in a multi-sensor scenario. Moreover, we presented four different noise parameter adaptation approaches. We evaluated our adaptation procedures in different simulation scenarios and compared our approach to state-of-the-art adaptive KFs. The evaluations show some superior aspects of our proposed adaptation as well as its performance and flexibility in the application areas.

In future work, we want to extend our framework to combine multiple-model adaptive estimation with a focus on process noise and our SL adaptation approach focusing on measurement noise. Furthermore, we want to extend our framework to nonlinear filtering and multi-object tracking.

References

[1] R. E. Kalman, “A new approach to linear filtering and prediction problems,” *Transactions of the ASME - Journal of Basic Engineering*, vol. 82, no. 1, pp. 35–45, 1960.

[2] R. Mehra, “Approaches to adaptive filtering,” *IEEE Transactions on Automatic Control*, vol. 5, pp. 693–698, 1972.

[3] S. Akhlaghi, N. Zhou, and Z. Huang, “Adaptive adjustment of noise covariance in kalman filter for dynamic state estimation,” in *2017 IEEE power & energy society general meeting*. IEEE, 2017, pp. 1–5.

[4] Z. Xian, X. Hu, and J. Lian, “Robust innovation-based adaptive kalman filter for ins/gps land navigation,” in *Proceedings - 2013 Chinese Automation Congress, CAC 2013*. IEEE Computer Society, 2013, pp. 374–379.

[5] K. R. Hamid, A. Talukder, and A. K. Ehtesanul Islam, “Implementation of fuzzy aided kalman filter for tracking a moving object in two-dimensional space,” *International Journal of Fuzzy Logic and Intelligent Systems*, vol. 18, no. 2, pp. 85–96, jun 2018.

[6] O. Kost, J. Duník, and O. Straka, “Measurement difference method: A universal tool for noise identification,” *IEEE Transactions on Automatic Control*, vol. 68, no. 3, pp. 1792–1799, 2022.

[7] J. Duník, O. Straka, O. Kost, and J. Havlík, “Noise covariance matrices in state-space models: A survey and comparison of estimation methods — part i,” *International Journal of Adaptive Control and Signal Processing*, vol. 31, no. 11, pp. 1505–1543, 2017.

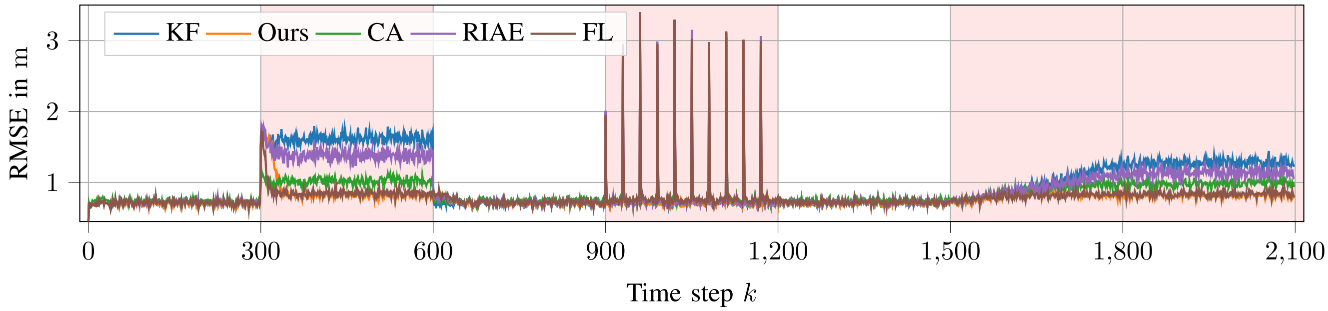

Fig. 5. Results of the adaptation methods in the measurement noise disturbance scenario of sensor 1. The adaptation methods aim to reduce the positional RMSE. The red shadows indicate the disturbance intervals.

TABLE I

Results of the adaptation methods in terms of positional RMSE values in the measurement noise disturbance scenario.

Method (time steps)	**Averaged positional RMSE in m**						
	Before jump (0 – 300)	During jump (300 – 600)	After jump (600 – 900)	Outliers (900 – 1200)	After Outliers (1200 – 1500)	Drift (1500 – 1800)	After drift (1800 – 2100)
KF	0.697	1.618	0.700	0,892	0.700	0.979	1.276
SL (ours)	**0.697**	0.916	**0.717**	0,898	**0.706**	0.812	**0.819**
CA	0.741	1.023	0.745	**0,811**	0.746	0.891	0.986
RIAE	0.716	1.399	0.730	0,930	0.724	0.933	1.137
FL	0.713	**0.879**	0.731	0,953	0.722	**0.806**	0.837

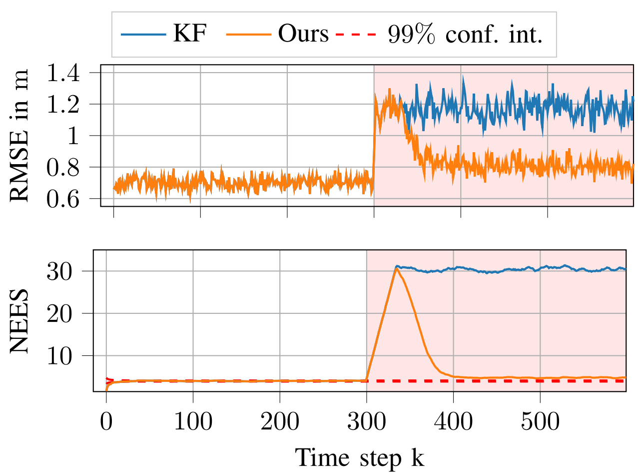

Fig. 6. The proposed SL adapter results compared to the KF in the process noise disturbance scenario. The adaptation method reduces the positional RMSE and keeps the time-averaged NEES within its confidence interval. The red shadow indicates the perturbation time interval.

[8] L. Zhang, D. Sidoti, A. Bienkowski, K. R. Pattipati, Y. Bar-Shalom, and D. L. Kleinman, "On the identification of noise covariances and adaptive kalman filtering: A new look at a 50 year-old problem," *IEEE Access*, vol. 8, pp. 59 362–59 388, 2020.

[9] P. He, B. Wang, and X. Liu, "Reinforcement learning adaptive kalman filter for ae signal's ar-mode denoise," in *2023 IEEE 11th International Conference on Information, Communication and Networks (ICICN)*, 2023, pp. 643–648.

[10] B. Boulkroune, K. Geebelen, J. Wan, and E. van Nunen, "Auto-tuning extended kalman filters to improve state estimation," in *2023 IEEE Intelligent Vehicles Symposium (IV)*, 2023, pp. 1–6.

[11] Y. C. e. a. C. Hu, W. Chen, "Adaptive kalman filtering for vehicle navigation," *Journal of Global Positioning Systems*, vol. 2, no. 1, pp. 42–47, 2003.

[12] T. Griebel, J. Müller, M. Buchholz, and K. Dietmayer, "Kalman filter meets subjective logic: A self-assessing Kalman filter using subjective logic," in *2020 IEEE 23rd International Conference on Information Fusion (FUSION)*. IEEE, 2020, pp. 1–8.

[13] T. Griebel, J. Müller, P. Geisler, C. Hermann, M. Herrmann, M. Buchholz, and K. Dietmayer, "Self-assessment for single-object tracking in clutter using subjective logic," in *2022 25th International Conference on Information Fusion (FUSION)*. IEEE, 2022, pp. 1–8.

[14] T. Griebel, J. Heinzler, M. Buchholz, and K. Dietmayer, "Online performance assessment of multi-sensor kalman filters based on subjective logic," in *2023 26th International Conference on Information Fusion (FUSION)*. IEEE, 2023, pp. 1–8.

[15] A. Jøsang, *Subjective Logic: A Formalism for Reasoning Under Uncertainty*. Springer International Publishing, 2016.

[16] Y. Bar-Shalom, X. R. Li, and T. Kirubarajan, *Estimation with Applications to Tracking and Navigation: Theory Algorthims and Software: Theory Algorithms and Software*. John Wiley & Sons, 2001.

[17] Y. Ho and R. Lee, "A bayesian approach to problems in stochastic estimation and control," *IEEE transactions on automatic control*, vol. 9, no. 4, pp. 333–339, 1964.

[18] A. P. Dempster, "Upper and lower probabilities induced by a multivalued mapping," *The Annals of Mathematical Statistics*, vol. 38, no. 2, pp. 325–339, 1967.

[19] G. Shafer, *A Mathematical Theory of Evidence*. Princeton University Press, 1976, vol. 42.

[20] A. Jøsang, D. Wang, and J. Zhang, "Multi-source fusion in subjective logic," in *2017 20th International Conference on Information Fusion (FUSION)*. IEEE, 2017, pp. 1–8.

[21] R. W. Van Der Heijden, H. Kopp, and F. Kargl, "Multi-source fusion operations in subjective logic," in *2018 21st International Conference on Information Fusion (FUSION)*. IEEE, 2018, pp. 1990–1997.

[22] R. W. van der Heijden, S. Dietzel, T. Leinmüller, and F. Kargl, "Survey on misbehavior detection in cooperative intelligent transportation systems," *IEEE Communications Surveys & Tutorials*, vol. 21, no. 1, pp. 779–811, 2018.

[23] A. Jøsang, J. Zhang, and D. Wang, "Multi-source trust revision," in *2017 20th International Conference on Information Fusion (FUSION)*. IEEE, 2017, pp. 1–8.

[24] Y. C. e. a. C. Hu, W. Chen, "Adaptive kalman filtering for vehicle navigation," *Journal of Global Positioning Systems*, vol. 2, no. 1, pp. 42–47, 2003.

[25] B. Hongwei, J. Zhihua, and T. Weifeng, "Iae-adaptive kalman filter for ins/gps integrated navigation system," *Journal of Systems Engineering and Electronics*, vol. 17, no. 3, pp. 502–508, oct 2006.